11,12,13,93

CERN/SI/Int. DL/71-8
17.9.1971

POTENTIAL BEAM BLOW-UP IN THE CERN PS BOOSTER DUE TO UNAVOIDABLE MAGNET IMPERFECTIONS AND CORRECTIVE MEASURES PROVIDED

C. Bovet, G. Guignard*), K.H. Reich and K. Schindl

Paper discussed by the Panel on "Limitations on beam quality and intensity" at the VIIIth International Conference on High Energy Accelerators
Geneva, 20-24 Sept., 1971

Distribution :

List MPS-SI/1

POTENTIAL BEAM BLOW-UP IN THE CERN PS BOOSTER DUE TO UNAVOIDABLE MAGNET IMPERFECTIONS AND CORRECTIVE MEASURES PROVIDED

C. Bovet, G. Guignard*), K.H. Reich and K. Schindl

European Organization for Nuclear Research, Geneva, Switzerland.

1. Abstract and Introduction

Efficient use of the CPS beam on external targets, in the ISR, and in the 300 GeV accelerator requires high beam density (besides high intensity), and hence a PSB[1] beam of good quality. While various collective effects are a major obstacle in reaching this goal, "zero-intensity" effects have required a roughly equal share of study and corrective measures. Among these effects, unavoidable magnet imperfections are preponderant, the rest resulting from mismatch at injection and transfer, gas scattering, power supply ripple, etc.

Magnet imperfections considered are (i) statistical fluctuations of the bending field B_0 and of the field gradient B', (ii) ring to ring variations of $\int_0^C B_0\, ds$, (iii) skew quadrupole fields, and (iv) higher order fields. As long as one stays away from the corresponding stop bands in the $Q_H - Q_V$ diagram, imperfections (i), (iii) and (iv) lead to distortions of the phase plane "ellipses" and to coupling between the two transverse planes rather than to actual beam blow-up. Nevertheless, we attempt to reduce the effects of all imperfections listed in order to be less restricted in the choice of Q_H, Q_V, to suffer a minimum dilution in six-dimensional phase space at the transfer into the CPS, and to facilitate PSB measurements and operation in general.

The desirable upper limits of the multipole coefficients up to order four are discussed. In some cases they are exceeded in practice and the corrective measures provided are described.

2. Magnet imperfections and their effects

2.1 The PSB magnet system

In each of the four rings, the magnet system (Fig. 1) consists of 32 main bending magnets, 16 F-D-F quadrupole triplets, 17 correction and steering dipoles (H + V), 20 multipole lenses, and a number of special magnets for beam injection and ejection and beam measurements.

Because of the emphasis on beam quality, the main magnet should produce dipole and quadrupole fields of high purity. A separate function magnet was chosen for the PSB, notably because it produces less unwanted field terms and more experience exists as to their correction than in the case of a combined function magnet[2]. However, and despite a very careful design and production[3], the magnet units exhibit some unavoidable imperfections.

In order to understand more easily the origin of these imperfections, to evaluate their effects on the beam, and to specify any correction elements required, the fields produced by the PSB magnet system are expressed**) by means of multipole coefficients a_n and b_n[6]:

$$\vec{B} = \sum_{n=1}^{\infty} r^{n-1} \left\{ \left[-a_n \sin(n-1)\phi - b_n \cos(n-1)\phi \right] \vec{i}_x + \left[-a_n \cos(n-1)\phi + b_n \sin(n-1)\phi \right] \vec{i}_z \right\}, \qquad (1)$$

where $r = \sqrt{x^2 + z^2}$, $\phi = \tan^{-1}(z/x)$, and n is the order of the coefficients (2n = number of poles).

2.2 Closed orbit

Focusing by lens triplets was chosen, mainly because it reduces the height of the gaps of the bending magnets and facilitates beam injection and ejection[1]. However, it requires stronger lenses than used in a FODO lattice and hence stricter alignment tolerances (Table 1) for the same closed orbit amplitude. (Contrariwise, the alignment of the bending magnets becomes uncritical.)

2.3 Stop bands

The existing theory was developed to be applicable to all stop bands occuring in an AG synchrotron[7]. For each of the N + 1 resonances of order

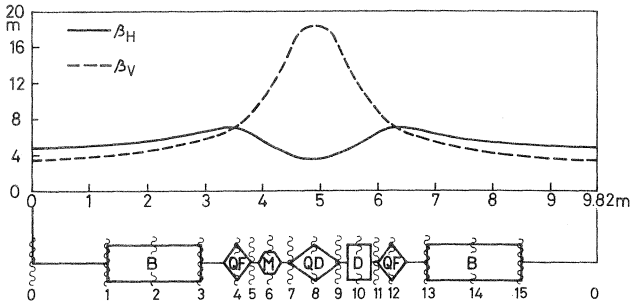

Fig. 1 - One of the 16 PSB lattice periods with β-functions and location of field imperfections.

Location	Field imperfection due to
1, 3, 13, 15	bending magnet (B) end field
2, 14	bending magnet central field
4, 8, 12	quadrupole (QF, QD) field
5, 7, 9, 11	unsymmetric coil connection
6	multipole correction lenses (M)
10	correction and steering dipoles (D)
0	multipoles, dipoles, septum magnet stray field, IBS field.

*) Present address: SIN, Zürich, Switzerland.

**) In the case of dipole magnets the coefficients are found from a least square fit of the measured $B_z(x)$ curves[4]; in the lenses, they are directly measured with a harmonic coil[5].

Table 1 - PSB multipole coefficients at 800 MeV [Measured values for half the B.'s and ¼ of the Q.'s in ( ).]

Element (Fig. 1)	$\int_0^{\mathcal{C}} \lvert a_1 \rvert ds$ [Tm]	$\Delta a_{1\ st}$ a) [Tm]	$\int_0^{\mathcal{C}} \lvert a_2 \rvert ds$ [T]	$\Delta a_{2\ st}$ a) [T]	$\int_0^{\mathcal{C}} \lvert b_2 \rvert ds$ b) [T]	$\Delta b_{2\ st}$ a) [T]	$\int_0^{\mathcal{C}} \lvert a_3 \rvert ds$ [T/m]	$\Delta a_{3\ st}$ a) [T/m]	$\int_0^{\mathcal{C}} \lvert a_4 \rvert ds$ [T/m²]	$\Delta a_{4\ st}$ a,c) [T/m²]
B	30.67 (30.67)	< 0.002 (0.005)	< 0.1 (0.06)	< 0.0021 -	< 0.005 (0.04)	< 0.0027 -	- (0.5)	< 0.87 -	- (10)	< 8.7 -
$Q_F + Q_D$	0.01 -	< 0.003 (0.012) d)	116 (116)	0.0008 (0.06)	< 0.003 (0.08)	< 0.0023 -	- (0.3)	< 0.43 -	- (7)	< 5.3 -
D + M e)	0.17	-	0.4	-	0.2 + 0.1	< 0.0014	19 f) +1.1	< 0.28	227 f) +13	< 3.0

a) $\Delta a_{n\ st} = \left[n_{e\ell} \sum_1^{n_{e\ell}} \left(\Delta \int_0^{\ell_{e\ell}} |a_n| ds \right)^2 \right]^{\frac{1}{2}}$ { Δa_1 results from closed orbit considerations; for $n \geq 2$ the Δa_n figures apply to $\Delta a_n = 0$ in the other elements; $\mathcal{C}$ = PSB circumference.

b) Determined from computer simulation (see Appendix).
c) At 50 MeV, since this is more critical because of larger beam emittance.
d) Originating from 0.1 mm r.m.s. displacement of magnetic axes in horizontal plane.
e) General-purpose sextupole and octupole lenses + specific correction elements of Table 2.
f) At 50 MeV and for a few mm closed orbit amplitude these values would be limited to a fraction of the figures given if the stop bands: $2\,Q_{H,V} = 9$ and $Q_H + 2\,Q_V = 13$ were not narrowed down.

$N(= n_1 + n_2)$ up to $N = 5$ the stop band widths $\Delta e = \Delta(n_1 Q_H + n_2 Q_V - p)$ are expressed explicitly in terms of the machine radius, the magnetic rigidity of the particles, the initial beam emittance ε_H, ε_V, and the azimuthal Fourier components of the field perturbations.

Disregarding any self-stabilisation due to amplitude-dependent frequency shifts, the maximum amplitude growth $g = y_{max}/y_0$ is found by determining the upper limit of the integral $(n_1 \neq 0)$

$$\left(\frac{\varepsilon_{V_0}}{\varepsilon_{H_0}}\right)^{n_2/2} \int_1^{g_x} \frac{dg}{g_x^{n_1-1} \left[\frac{\varepsilon_{V_0}}{\varepsilon_{H_0}} + \frac{n_2}{n_1}(g_x^2 - 1)\right]^{n_2/2}}$$

$$= \frac{\pi\, \Delta e}{\left(n_1 + \frac{n_2^2}{n_1}\frac{\varepsilon_{H_0}}{\varepsilon_{V_0}}\right)\left(n_1 |\Delta Q_{H\ rev}| + n_2 |\Delta Q_{V\ rev}|\right)^{\frac{1}{2}}} \quad , \quad (2)$$

and similarly for g_z, where ΔQ_{rev}, the mean Q change per revolution, is taken to be

$$\Delta Q_{rev} = 4\, Q_s\, \Delta \hat{Q} \qquad (3)$$

with $\Delta\hat{Q}$ as the amplitude of the periodic Q variation (due to synchrotron oscillations) and Q_s the (fractional) number of synchrotron oscillations per turn. For n_R stop band crossings the amplitude increase is $(n_R/2)^{\frac{1}{2}}$ times greater.

The excitation of second and third order resonances through a combination of the 16th sextupole (resp. octupole) harmonic and the 7th (resp. 2nd and 3rd) closed orbit harmonic is also considered.

The trim supplies connected in parallel to the main quadrupoles permit the shifting of the Q value at a rate $\dot{Q}$. Stipulating that on average the amplitude growth should stay below 5% during the crossing of a stop band leads to the tolerances listed in Table 1.

2.4 Effects outside stop bands

A computer simulation of the PSB is used to study these effects (see Appendix). The imperfections of all elements are introduced as equivalent thin lenses placed at the appropriate points in the PSB lattice. In the case of the bending magnets three thin lenses are used (Fig. 1). In the case of the quadrupoles the single thin lens introduced for simplicity leads to slightly pessimistic results. The total emittance variation in the V plane resulting from all measured imperfections is shown in Fig. 2a. At injection one has $\Delta\varepsilon_H = 29 \times 10^{-6}$ rad m and $\Delta\varepsilon_V = 33 \times 10^{-6}$ rad m.

2.5 Effects due to magnet differences from ring to ring

In transverse phase space the effects of the bending magnets concern mainly the matching at injection into the PSB and at transfer into the CPS. To simplify PSB operation and to save cost, each set of four injection and four ejection septum magnets is powered and positioned as a unit. Under these conditions the respective closed orbits at these magnets must be made closely identical in the four rings if emittance blow-up is to be avoided.

Because of the strong influence on the closed orbit, a tolerance of ± 0.03 mm is specified on the gap-to-gap spacing of the geometric centres of each quadrupole unit.

In longitudinal phase space a difference in the

PSB guide fields leads to a dilution of the bunch area after capture in the CPS buckets. Negligible dilution (bunch area increase < 5%) requires $\int_0^C (\Delta B_0/B_0)ds \leqslant \pm 10^{-4}$ from ring to ring[8].

3. Corrective measures provided

In the case of both the straight bending magnets and the main quadrupoles the effect of imperfections located inside these units cannot be corrected well outside because of the change of the amplitude function (Fig. 1) and the proton trajectories.

Therefore, in both cases, the policy was to make the fields inside these elements as ideal as possible and to correct the end fields by local shimming. In the case of the bending magnets, advantage was taken of this individual shimming of each gap to reduce the statistical fluctuations of $\Delta a_{1\ st}$[3]. For the main quadrupoles, use of a single lamination for all lens units and support of the triplet by a common girder were adopted to meet the very stringent alignment requirements of the magnetic axes. All free long straight sections are magnetically shielded to reduce random fields to 10^{-5} T[9]. All the same, some of the tolerances aimed at in Section 2 remained unattainable and corrective measures became indispensable.

A total of six sets of correcting elements will be available[10] (Table 2). A correction winding in the bending magnets is used to equalize the four integrals $\int_0^C B_0 ds$ from ring to ring. The pulsed power supplies are controlled and programmed by computer[11].

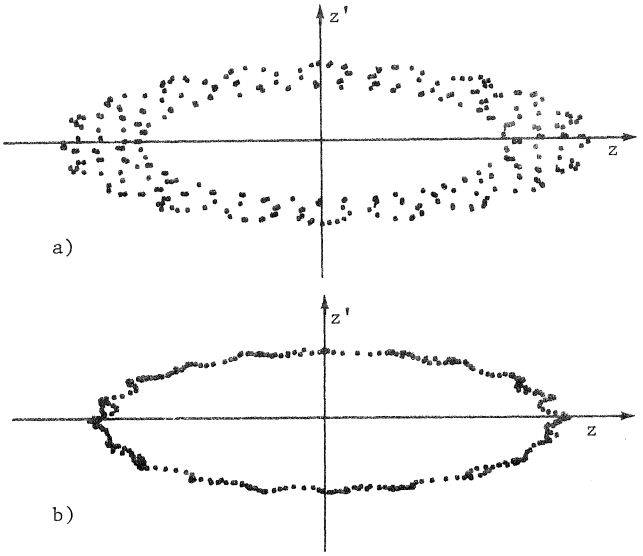

Fig. 2 - Large amplitude particle trajectory in vertical phase plane under the influence of the PSB magnet imperfections at 50 MeV (the particle position after every lattice period is represented by a dot; $\varepsilon_{H_0} = 130 \times 10^{-6}$ rad m, $\varepsilon_{V_0} = 40 \times 10^{-6}$ rad m).

a) Situation for optimized magnet design.
b) Improved arrangement of power cable connections and skew quadrupole compensation ($\int_0^C b_2\ ds$ = - 0.016 T).

Table 2 - PSB closed orbit and stop band correction elements[10] (excluding the 4 + 3 dipoles for orbit deformation at injection and ejection, and the 16 general-purpose sextupole and octupole lenses at location 6 of Fig. 1).

Type of element	Locat. (Fig.1)	Number per ring	Indep. contr./r.	Strength[a]	Correction of
Dipoles	10 + 0	(16 + 1)H,V	17 + 17	0.17 Tm	closed orbits
Quad.'s	0 + 6	(2 +2)p.'s[b]	4[c]	0.4 T	$2Q_{H,V} = 9$
Skew Q.'s	6	8	1	0.2 T	$Q_H - Q_V = 0$
	6	2 pairs[b]	2	0.1 T	$Q_H + Q_V = 9$
Sextup.'s	0	2 pairs[b]	2	1.1 T/m	$n_1Q + n_2Q = 14$
Octup.'s	0	2 pairs[b]	2	13 T/m^2	$n_1Q + n_2Q = 19$

a) $\int_0^C |a_n|ds$ ($\int_0^C |b_n|ds$ in the case of the skew quadrupoles)
b) In-pair phase shift to give the wanted p^{th} harmonic, pair-to-pair shift to give sin pθ and cos pθ terms
c) These four controls are combined by software to allow independent tuning in either plane.

The orbit correction[7] is based on the analysis of its eigenvectors and the minimization of the correction currents. Besides the usual aim of saving magnet aperture, the design of the orbit correction system was guided by the wish to minimize injection and ejection errors. An analytical study showed that the number of correcting dipoles should be between 2Q and 3Q in order to provide a good compromise between money invested and results obtained. This was confirmed by a detailed numerical study[7], and 16 dipoles were placed at location 10 and 16 orbit observation stations at location 6 of Fig. 1.

At injection, the closed orbit will be corrected with special care in the injection region where two extra orbit observation stations are installed (close to locations 1 and 3 of Fig. 1). At transfer, two special dipoles are used for each plane in each ring allowing independent control of the closed orbit at the ejection septum magnet.

As regards the situation presented in Fig. 2a, closer analysis showed that a substantial skew quadrupole contribution comes from the unavoidable asymmetry of the power cable connections to the main quadrupoles (having an excitation winding of only two turns per pole). A noticeable improvement resulted from connecting half the lenses at the upstream (U) end and half the lenses at the downstream (D) end, following a patern UDUD for F lenses and UUDD for D lenses. The situation is further improved (Fig. 2b) by the use of the skew correction quadrupoles, leading to $\Delta\varepsilon_H = 11 \times 10^{-6}$ rad m and $\Delta\varepsilon_V = 12 \times 10^{-6}$ rad m.

To optimize the use of the various correction magnets, powerful instrumentation is provided[12], notably for non-destructive orbit and beam profile observation, and Q measurements.

4. Conclusions

The computer simulation of the beam behaviour has made available a "yardstick for magnet quality", more usually provided by the particles once circulating. At all stages of the magnet design and pro-

duction this "yardstick" has contributed to the obtaining of the remarkable quality of the PSB magnet system, and the concomitant lessening of potential beam blow-up.

Nevertheless, because of the stringent beam quality requirements for this injector synchrotron, it is indispensable to correct carefully the closed orbit and to narrow down certain stop bands. Refined analytical and numerical studies led to the result that less dipoles and orbit observation stations and more multipole correction lenses were required than thought initially.

While some of the problems encountered and the measures taken are specific to the PSB, most are applicable to other synchrotrons. In particular, skew quadrupole corrections seem unavoidable, while orbit correcting dipoles may possibly be dispensed with in a synchrotron using a separate function magnet with individually shimmed units.

Acknowledgements

It is a pleasure to acknowledge the excellent collaboration we enjoy with the SI Magnet Group from which this work greatly benefited.

Appendix

Computation of emittance variation due to magnet imperfections

In either transverse phase plane, the emittance of the beam may be related to the Courant-Snyder invariant

$$W = \beta(s)y'^2(s) + 2\alpha(s)y(s)y'(s) + \gamma(s)y^2(s) \qquad (A1)$$

for the particle with the largest betatron amplitude. In a linear synchrotron this quantity is constant, whereas in the presence of non-linear fields, W varies by some ΔW. When circulating in a perturbed machine the beam will occupy a phase space area $\pi(W + \Delta W)$. At transfer into another machine the emittance will be blown up by an amount $\Delta\varepsilon \leqslant \Delta W$ since matching is achieved only for the linear part of the field.

In order to calculate ΔW, the coordinates y(s), y'(s) of one large amplitude particle are traced through the simulated PSB[4]. The linear magnetic elements are treated by 2 x 2 matrix transformations[13]. The perturbation fields are introduced as thin lenses (Fig. 1) giving rise to deflections (e.g. in the horizontal plane)

$$\Delta x'(x,z) = \frac{\ell_e}{B_0\rho}\,\Delta B_z(x,z) \ , \qquad (A2)$$

where ℓ_e is the effective length of the element with a perturbation ΔB_z.

The values of $\Delta x'$ obtained for the bending magnet with three thin lenses agree closely with those found by Runge-Kutta integration of the actual trajectory[14]. In order to avoid variation of W due to discontinuities of the field derivatives occuring when a measured field map is used, the field imperfections are represented by means of harmonic functions [Eq. (1)]. The multipole coefficients a_n and b_n are obtained by a least square fit to the measured field map up to an order such that the standard error of the approximation corresponds to the measurement accuracy.

Since the closed orbit in the PSB is not yet known, stochastic misalignments are generated by 96 dipoles powered at random, giving rise to a r.m.s. closed orbit distortion of the order of 20 mm. Computation is then performed for many different orbits.

For a particular working point Q_H, Q_V, and given dipole strengths, the computation of ΔW proceeds in the following steps:

i) determine the closed orbit $x_c(s)$, $x_c'(s)$, $z_c(s)$, $z_c'(s)$, taking into account the dipole strengths and the field perturbations under study;

ii) compute the Twiss parameters $\alpha_c(s)$, $\beta_c(s)$, $\gamma_c(s)$ by analyzing a small amplitude trajectory around the closed orbit;

iii) calculate for a large number of revolutions the function

$$W(s) = \beta_c(x' - x_c')^2 + 2\alpha_c(x - x_c)(x' - x_c') + \gamma_c(x - x_c)^2$$

(and similarly for the vertical plane) with the initial conditions

$$x(0) = \sqrt{\frac{\varepsilon}{\gamma_c(0)}} + x_c(0) \ , \qquad x'(0) = x_c'(0).$$

The largest emittance variation is then

$$\Delta\varepsilon \leqslant \max\left[W(s)\right] - \min\left[W(s)\right] . \qquad (A3)$$

References

1) C. Bovet, K.H. Reich, Proc. 6th Int. Acc. Conf., Cambridge, 1967 (CEA, Cambridge, 1967), p. 315.

2) G. Danby, J. Allinger, J. Jackson, IEEE Trans. Nuclear Sci. NS-14, 431 (1967).

3) A. Asner et al., Proc. 3rd Int. Conf. on Mag. Techn. Hamburg 1970, and private communication.

4)* C. Bovet, K. Schindl, SI/Int. DL/70-4.

5)* K. Lohmann, C. Iselin, SI/Note MAE/69-18 Rev. 1.

6)* G. Brianti, SI/Note DL/71-3.

7) G. Guignard, CERN 70-24.

8)* U. Bigliani, MPS/Int. RF/B 67-12.

9)* H. Koziol, SI/Note DL/68-22.

10)*C. Bovet, K.H. Reich, SI/Int. DL/69-3 and SI/Note DL/70-8.

11) E. Asseo et al., IEEE Trans. Nuclear Sci. NS-18, 354-358 (1971), (Chicago Conference).

12) H. Koziol, K.H. Reich, IEEE Trans. Nuclear Sci. NS-18, 347-351 (1971), (Chicago Conference).

13)*C. Bovet, BOOM, SI/Note DL/69-17.

14)*C. Bovet, K. Schindl, SI/Int. DL/71-2.

*) CERN Internal report or note.